Recent Studies on Digestive System Anatomy

Chapter 2

Endoscopic Microanatomy of the Human Gastrointestinal Mucosa

Hugo Uchima[2]*; Kenshi Yao[1]

[1]Department of Endoscopy, Fukuoka University Chikushi Hospital, Fukuoka, Japan.

[2]Department of Endoscopy, Teknon Medical Center, Barcelona, Spain

Correspondence to: Hugo Uchima, *Department of Endoscopy, Hospital Universitari Doctor Josep Trueta,*

Girona, Spain.

Ph: +34 972 940 200 - 2287; E-mail: huchima.girona.ics@gencat.cat

Abstract

Dual wavelength imaging with bandwidth narrowing is an image-enhanced endoscopy technology based in the interaction of narrow band spectrum of light with the mucosal surface and the hemoglobin of the microvasculature.

Narrow-band imaging (NBI) , blue light imaging (BLI) and Optical enhancement (OE) are examples of this technology.

The study of the microsurface structure and the microvascular architecture of the gastrointestinal mucosa have medical implications, specially in the diagnosis and characterization of early neoplastic lesions allowing a treatment with organ preservation.

Abbreviations:

BLI: blue light imaging / blue laser imaging; EGJ: esophagogastric junction; IPCL: intrapapillary capillary loops; DWI: dual wavelength imaging with bandwidth narrowing; M-DWI: magnifying endoscopy with dual wavelength imaging; ME: magnifying endoscopy; WLI: white light-imaging; MS: microsurface; MV: microvascular; NBI: narrow band imaging; OE: optical enhancement; SEC: subepithelial capillaries

1. Introduction

The gastrointestinal tract has special medical interest because it might harbor a wide variety of pathologies. For instance, in the USA, gastrointestinal diseases impact on a currently estimated at 60-70 million people annually being a source of substantial burden and cost with colorectal cancer as the leading cause of death in this group of diseases [1].

Likewise, in developing countries, the burden of gastrointestinal, liver, and pancreatic diseases has been increasing [2]. According to WHO, from 2000 to 2015, gastrointestinal tumours are in the top 20 causes of worldwide mortality with colorectal cancer in the third and gastric cancer in the fifth place for both sexes [3].

At a present time (2017), in Spain and Japan colorectal cancer is the most frequent cancer affecting men and women, followed closely by gastric cancer in Japan [4].

With flexible endoscopy, studying the gastrointestinal tract has evolved progressively leading to a better understanding of the diseases improving diagnosis, characterization and treatment of early gastrointestinal tumours regarding organ preservation [5,6,7].

Last decade, the technological progress led to the development of better endoscopic imaging giving the endoscopists the possibility to study the microvasculature and microstructure of the gastrointestinal tract *in vivo*. Because of that, gastrointestinal endoscopy has now a crucial role in the diagnosis and management of early gastrointestinal tumours.

We will review the basics of the microanatomy of the gastrointestinal mucosa evaluated by magnified and non-magnified endoscopy using the optical narrow band technologies.

2. Dual Wavelength Imaging with Bandwidth Narrowing / The Narrow Band Technology

Wave-particle duality is one of the characteristics of light. Visible light for the human eye is electromagnetic radiation within a certain portion of the electromagnetic spectrum, usually defined as having wavelengths (the distance between peaks in each wave) in the range of 400–700 nanometres (nm), between the infrared (with longer wavelengths) and the ultraviolet (with shorter wavelengths). This wavelength means a frequency range of roughly 430–750 terahertz (THz). The spectral sensitivity of the light-adapted eye depends on the photo pigments in the three kinds of cones (with a different absorbance spectrum), called S, M and L (for short, medium, and long wavelengths, ~420, 530, and 560 nm), the longer wavelength will be seen as red, with the shorter as blue, and in between as green [8,9].

The biological pigments in the human body can be divided into hematogenous pigments (as hemoglobin), non hematogenous pigments (as melanin) and endogenous minerals (as copper) [10]. Hemoglobin is composed of a single protein called globin and a compound called "heme" , the latter containing iron atoms and the red pigment porphyrin (a metalloporphyrin). The absorption of visible light in metalloporphyrins take place at wavelengths around 400 nm ("blue light") and 550nm ("green light"), reflecting the "red light" (wavelengths around 700nm), giving the color to blood (**Figure 1**). If red light is omitted and only the dual wavelengths green and blue are projected directly to the hemoglobin, it will absorb the blue and

green light and no light would be reflected, giving the perception of black [11].

One of the most important advances in the field of endoscopic imaging last decade has been the introduction of the dual wavelength imaging with narrow band technology. This technology first developed by Olympus Medical Systems Corp in collaboration with National Cancer Center Hospital East (Tokyo, Japan), known as narrow band imaging (NBI) is an optical digital method of image-enhanced endoscopy based in the narrow band spectrum of light and its effects on the mucosal surface and the hemoglobin of the microvasculature [12,13].

The gastrointestinal mucosa is a semitransparent medium (optical turbid) with small particles (complex proteins, and cell structures), when light strikes this particles, it diffuses (scattering). Different light wavelengths have different reflection, depth of propagation, and scattering in the biological tissue (**Figure 2**). Red light diffuses widely and deeply because of its longer wavelength, compared to blue light that has a short wavelength and propagates shallowly and is scattered over a narrow area.

NBI functions by filtering the illumination light eliminating the red component and by narrowing from 50-70nm to 20-30nm the spectral bandwidth of the blue (centered on 415nm) and green (centered on 540m) light, giving a dual wavelength imaging with bandwidth narrowing that can visualize capillary networks clearly. The narrow band blue light delineates in high contrast superficial microvessels, and narrow band green light, that penetrates the tissue over a fairly deep and fairly wide range, delinates in high contrast vessels in the middle layers. The incoming signals (from the charge-coupled device, CCD) from the camera of the endoscope are then combined by the video processor doing specific color allocation to produce a final color image (the narrow band blue image is allocated to the blue and green color channel and the narrow band green image is allocated to the red channel). On the NBI image displayed, the more superficial thin capillary network underneath the epithelium has a brownish appearance and thick deeper blood vessels have a cyan appearance (**Figure 3**).

Since its launch in 2005, NBI with high definition or magnifying endoscopes has been used worldwide by gastrointestinal endoscopist to improve visualization of the vascular patternsin the superficial part of the mucosa for a better diagnosis, predicting histology, distinguishing between neoplasia and non-neoplasia, and depth of infiltration of early gastrointestinal tumors. Nowadays, new systems similar to NBI, the BLI (blue light imaging in Europe and blue laser imaging in Japan, Fujifilm) and OE (Optical Enhancement system, Pentax) are also available and seems to be very useful in clinical practice as well [13-17].

3. Endoscopic Gastrointestinal Microanatomy

Endoscopic imaging has been evolving, and now-a-days, there are available different endoscopes with high magnification (>100x) and high resolution power, varying according

to manufacturers. If we define the maximal endoscope's resolution as the size of the smallest structure that can be visualized when the endoscope has been brought as close as possible to the object while staying in focus, for targeting the capillaries (microvessels) a resolution of at least 8um is required [18,19].

With the use of dual wavelength imaging with bandwidth narrowing, magnifying endoscopy allows the endoscopist an in *vivo* study of the microanatomy, by observing the microsurface and the microvascular architecture, even the red blood cells movement using the maximal resolution power of a high-definition magnification endoscope.

For performing this examination, the use of hood at the tip of the endoscope to fix the distance to the mucosal surface is helpful in order to consistently focus the microstructures at maximal resolution power [19].

Then we will review the endoscopic microanatomy of the mucosa of the esophagus, stomach, small bowel (duodenum and ileum) and large bowel, with magnifying endoscopy (ME) and dual wavelength imaging with bandwidth narrowing, that we will refer as dual wavelength imaging (DWI). The recognition of the microsurface (MS) structure and microvascular (MV) architecture has biological significance and medical implications, specially in the characterization of early gastrointestinal neoplasia, because both the neoplastic vessels and epithelium undergo considerable change during progression to invasive cancer [20].

4. Endoscopic Microanatomy of the Esophageal Mucosa

During white light-imaging (WLI) evaluation the esophageal mucosa appears smooth and pink, and the esophagogastric junction (EGJ) appears as an irregular Z-line (ora serrata) demarcating the interface with the redder gastric mucosae. The longitudinal palisade vessels, are relatively large vessels more frequently in the lamina propria rather than in the submucosa at the lower oesophageal sphincter, they are visible at endoscopy and helpful in defining the oesophagogastric junction.

The esophageal mucosa, about 500-800 um thick, is composed of non-keratinising stratified squamous epithelium (300-500um), with a subjacent lamina propria resting on the underlying muscularis mucosae. There are numerous intraepithelial papilla projecting upwards for 2/3 of the total thickness of the epithelium containing intrapapillary vessels called intrapapillary capillary loops (IPCL) arising perpendicularly from the branching vessel network that is located immediately above the muscularis mucosa, in the lamina propria. The IPCL are end capillaries of about 7-10 μm (allow the passage of single red blood cells) that run adjacent to basement membrane, being affected by alterations in the basal or parabasal layer and reflecting morphological changes of the epithelial papilla. IPCL's morphological changes has an important role in the characterization of early squamous cell carcinoma [21,22,23].

The IPCL are identified as red dots under white light and as brown dots with dual wavelength imaging (DWI), and the branching vessels are red under white light and cyan under DWI. In **Figure 3** we can see this microvascular architecture by using magnifying endoscopy with dual wavelength imaging with bandwidth narrowing (M-DWI).

The observation of the microsurface structure has clinical implications in the study of Barrett's esophagus, a premalignant condition secondary to gastroesophageal reflux disease, because in this condition the normal squamous epithelium of the esophagus (smooth microsurface) is replaced by a columnar epithelium (**Figure 4a**). The changes in microsurface structure and microvascular architecture are predictors of dysplasia and risk of advanced Barrett's adenocarcinoma [24] as shown in **Figures 4b and 4c.**

5. Endoscopic Microanatomy of the Gastric Mucosa

The stomach is a J-shaped dilation of the alimentary canal, it begins at the gastric cardia (the portion that envelops the lower esophagus) with gradual histological transition from cardiac glands to the second region, the acid-secreting segment (fundus and body) and then to the final region, corresponding to the antrum and pylorus. The mucosa is lined by a simple layer of columnar epithelial cells (20 to 40 µm height), that invaginates into the mucosa increasing the surface area of the gastric lining, forming gastric pits (foveolae), which are shallowest in the cardiac region and deepest in the pyloric region. The gastric pits provide the gastric glands of the lamina propria acces to the gastric lumen (about 4 or 5 glands per pit).

Body and fundic mucosa have the same histology characterized by straight and simple tubular glands known as fundic (oxyntic) glands. This mucosal thickness varies from 400 µm to 1500 µm, with the ratio of pit and proper gland thickness being 1:2 in the gastric fundic gland mucosa and 1:1 in the gastric pyloric gland mucosa. Inmmediatly deep to the basement membrane of the epithelial layer lies the lamina propria, containing the subepithelial capillaries (SEC), arising from branch from submucosal arterioles penetrating the muscularis mucosa. The SEC are distributed from the base of the glands towards the epithelium as they repeatedly anastomose with each other surrounding the glands, forming a regular honeycomb like subepithelial capillary network (SECN) in the gastric fundic gland mucosa and a coil-shaped SECN in the gastric pyloric gland feeding into subepithelial collecting venules (CV). The CVs travel obliquely downwards within the lamina propria to the submucosal venules.

The narrow band blue light contributes to visualization of subepithelial capillary network (SECN) and the mucosal microsurface structure. The narrow band green light contributes to visualization of part of the SECN and to visualization of the collecting venules (CVs), located deeper than the subepithelial capillaries.

In the fundic gland mucosa, CVs are seen red under white light or cyan under DWI. Us-

ing M-DWI, the SECs are visualized as brownish polygonal (mainly hexagonal) closed loops of subepithelial capillaries anastomosing with each other, giving a of honeycomb-like pattern. The marginal crypt epithelium (MCE) is seen as a semitransparent white border surrounding the crypt opening (CO) which is seen as a dark brown oval-shaped hole. The area between crypt and crypt is called the intervening part (IP). An scheme and a picture of the normal pyloric glandular mucosa are shown in **Figures 5a and 6**.

The antrum and pylorus contains the extensively coiled pyloric glands. Mucosal capillaries are relatively sparse compared with the fundic gland mucosa. At the lamina propria, some capillaries branch straight from arterioles beneath the muscularis mucosa and some from arterioles that penetrate the muscularis mucosa and then branch out. Capillaries repeatedly anastomose with each other reaching the subepithelial region forming a coil-shaped subepithelial capillary network (SECN), and then feed into collecting venules (CVs) in a relatively deep part of the lamina propria.

In the gastric pyloric gland mucosa, CVs are difficult to discern even using M-DWI, because they are located deep to the superficial layer of the mucosa.

Using M-DWI, the SEC are visualized as brownish coil-shaped open loops, and rarely with a reticular pattern.

The microsurface structure of the gastric pyloric gland mucosa is made up of the marginal crypt epithelium (MCE) surrounding the intervening part (IP), the MCE morphology is usually polygonal but may be curved or linear. Crypt openings are not visualized in the antrum because crypts running perpendicular to the mucosal surface are uncommon [11,19,21,25,26]. An scheme and a picture of the normal pyloric glandular mucosa are shown in **Figures 5b and Figure 7.**

The Light blue crest sign (LBC, **Figure 8a**), described first by Uedo et al [26] is defined as a fine blue white line on the crests of the epithelial surface/gyri and it is an optical marker for the endoscopic diagnosis of intestinal metaplasia, being well correlated with histology. This phenomenon involves strong reflection of short wavelength narrow-band blue light, probably by the microvilli of the brush borders of the areas of intestinal metaplasia. The same phenomenon is seen in the epithelial margins of small bowel mucosa.

The white opaque substance (WOS, **Figure 8b**) is another phenomenon [27], visualized using either normal white light or blue light, and indicates the accumulation of lipid microdroplets in the superficial (intraepithelial and subepithelial) part of gastric epithelial neoplasias (adenoma and cancer), due to an impaired mitochondrial oxidation, lipoprotein excretion and lipid degradation. The lipid drops have a higher reflective index than organelles and organic components of the tissue, it follows that projected light is strongly scattered and reflected,

this strong backward scattering and reflection of light is recognized as white coloration by the human eye [28,29]. WOS is another optical marker for intestinal metaplasia as well as LBC [30].

Irregularity in microvascular and microsurface patterns are present within the demarcation line are predictors of gastric cancer (**Figure 9**) [31].

6. Endoscopic Microanatomy of the Mucosa of Duodenum and Ileum

The small bowel extends from the gastric pylorus to its insertion into the large intestine at the junction of the caecum and ascending colon.

The duodenum, the most proximal portion of the small bowel, was so named because it is approximately 12 fingers in breadth. It has a mucosa made up of a single layer epithelium, a supporting lamina propria and the muscularis mucosae. The epithelium and lamina propria form leaf-like (spade-like) intraluminal projections called villi (lining the entire small bowel), covered by a brush border at the apical surface, surrounded by tubular invaginations known as crypts of Lieberkühn, that extend to the muscularis mucosa. The lamina propria contains a centrally located lymphatic capillary (lacteal) and an arteriovenous capillary network.

The villi in the duodenal bulb (proximal part) have a distorted appearance and tend to be short, in contrast, the villi of the distal duodenum are tall, slender, and regular.

Under endoscopic examination with ME-DWI, the microsurface structure (S) shows a regular curved (if observed obliquely) or oval-shaped (if observed perpendicular) marginal villous epithelium (MVE), visualized as a white belt-like structure. Light blue crest (LBC) can be visualized in the periphery of the normal duodenal and ileal MVE, depending on the direction of the observation (reflection of the blue light).

The crypt openings normally are not visualized, because they are deeper than the villi

The microvascular (V) architecture shows loop-shaped capillaries located inside the villi bordering of the MVE forming anastomoses inside the villi, the regular villous subepithelial capillary network (V-SECN). At times they can be observed flowing into the villous venules (VV) in the deep part. **Figure 9a** [32].

In celiac disease, when there is atrophy of the duodenal villi, the disappearance of the microstructure becomes evident (**Figure 9b**) [33,34,35].

The terminal ileum shows a similar microsurface structure and microvascular architecture to the duodenum, **Figure 10**.

7. Endoscopic Microanatomy of the Mucosa Colon and Rectum

The mucosa of the large intestine is a relatively smooth surface characterized by the presence of crypts of Lieberkühn and composed of a simple columnar epithelium, lamina propria with capillaries and associated venules, and muscularis mucosa at the lower border. The crypts of Lieberkühn are tubular and dip to the muscularis mucosae, giving a "rack of test-tubes" appearance.

With high definition ME-DWI, it is possible to visualize a regular hexagonal or honeycomb-like subepithelial capillary network (SECN) in each part of the large intestine, except for the rectum [36] as seen in **Figure 11**.

In clinical practice, the study of the microcapillary pattern of colonic lesions identify neoplastic lesions and predict the grade of submucosal invasion [37,38,39] (**Figure 12**).

8. Figures
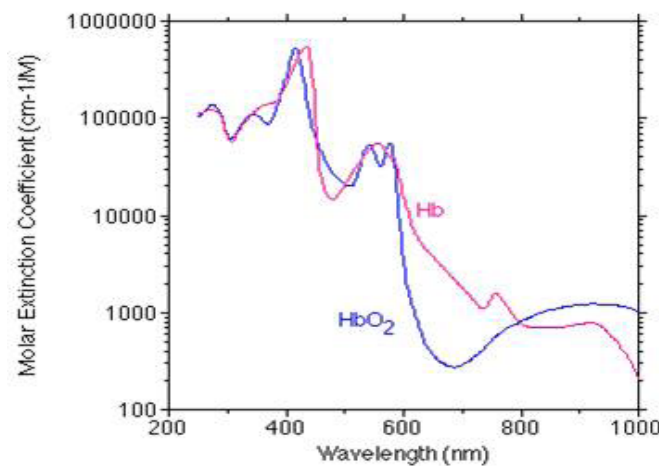
Figure 1: Optical Absorption Properties of Hemoglobin. The amount of light that is absorbed by oxy- and deoxy-hemglobin (blue and red lines respectively) at wavelengths from 400 nmthrough 900 nm. Absorption is higher around 400nm ("blue light") and 550nm ("green light") than around 700nm ("red light"). These graphs were generated from publicly available data on the web compiled by Dr. Scott Prahl, Oregon Medical Laser Center at http://omlc.ogi.edu/spectra/hemoglobin/summary.html, tabulated from data by Drs. W. B. Gratzer, Med. Res. Council Labs, Holly Hill, London and N. Kollias, Wellman Laboratories, Harvard Medical School, Boston.
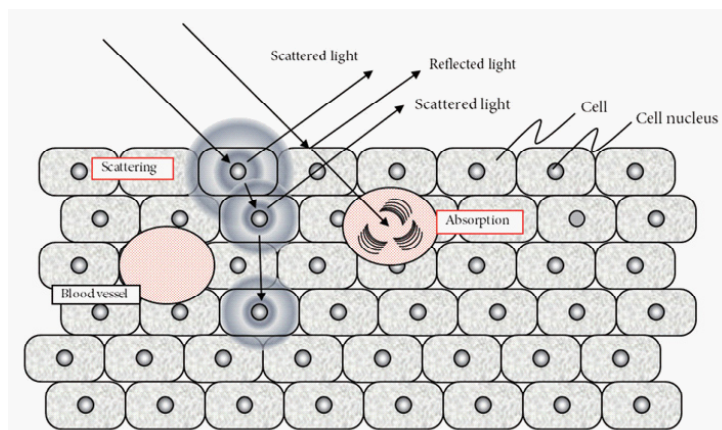
Figure 2: Scattering and absorption of light in a biological tissue. Multiple scattering occurs among light and small particles (cell nucleus and organelles), and light propagates diffusively, depending on its wavelength. Reproduced from Gono K, reference 12.
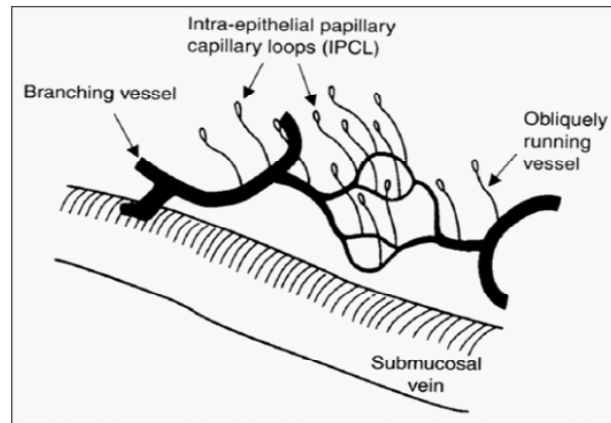
Figure 3a: Scheme showing the microvascular arquitecture of the mucosa, that drains in the submucosal vein. The IPCL run adjacent to basement membrane of the esophageal squamous epithelium, and can reflect morphological changes of the epithelial papilla, for example in cases of epithelial cancer (squeamous cell carcinoma). Figure reproduced from Inoue et al, [22].
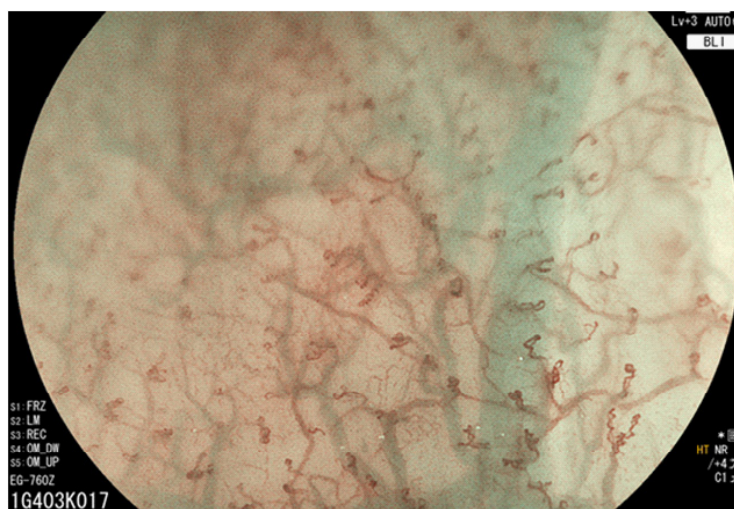

Figure 3b: Normal esophageal mucosa microanatomy under BLI (Blue light imaging, Fujifilm) magnifying observation. The Branching vessels are cyan, and the small capillaries are brown. The small capillaries form intrapapillary capillary loops (IPCL) at the level of the papilla beneath the epithelia. Picture Dr. Uchima, Teknon Medical Center.
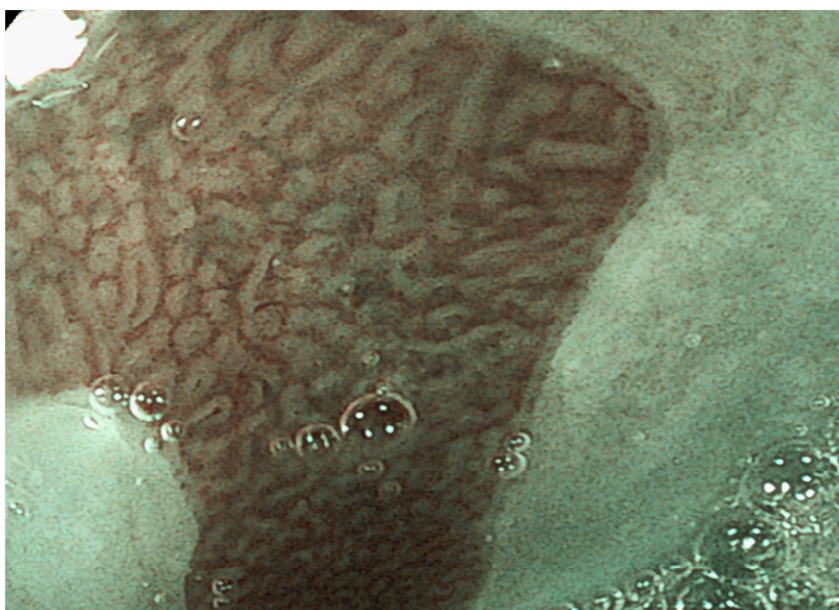
Figure 4a: Columnar-lined epithelium, known as Barrett's esophagus, is seen as brownish area in contrast to the whitish esophageal squamous epithelial around. The microsurface structure shows a round (circular) and tubular mucosal pattern without irregularities (no dysplastic Barrett's esophagus). BLI (blue-light imaging, Fujifilm) with medium magnification observation. Picture Dr. Uchima, Teknon Medical Center.
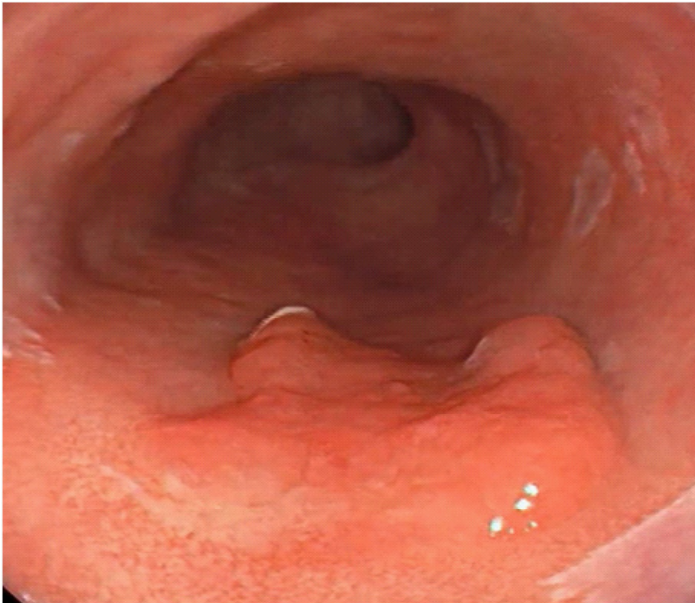
Figure 4b: White light observation showing a circumferential columnar epithelium in the lower esophagus (Barrett's), with a well demarcated elevated neoplastic lesion.

Figure 4.c. BLI (blue light imaging, Fujifilm) with high magnification of the same lesion. It is not possible to recognize glandular structures (irregular microsurface), only abrnormal microvessels. This was an adenocarcinoma with infiltration of the submucosal layer. Pictures from Dr. Uchima, Teknon Medical Center.
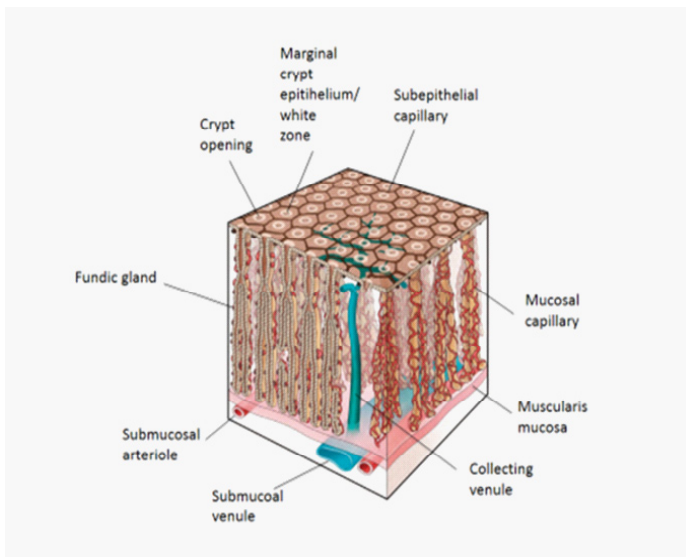

Figure 5a: Scheme of the normal microanatomy of the fundic gland mucosa. Notice the relation of the Crypt opening (CO), the marginal crypt epithelium (MCE) and the honeycomb-like subepithelial capillary network (SECN). The area between crypt and crypt is called the intervening part (IP). Scheme from Prof. Kenshi Yao, reference 31.
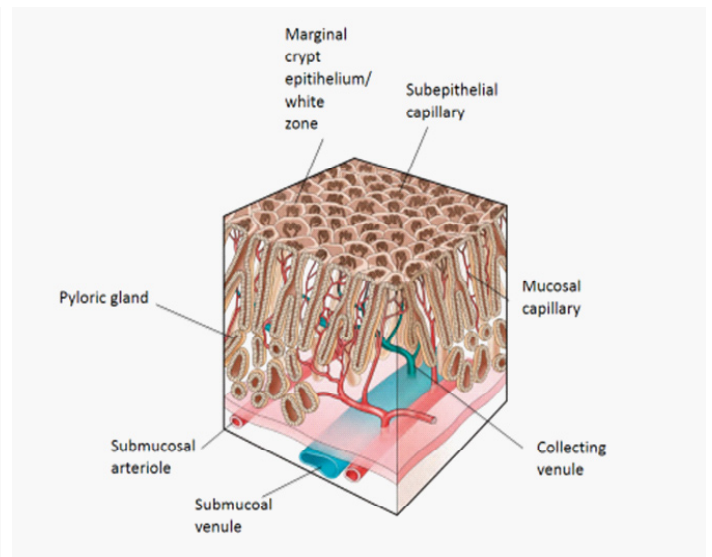
Figure 5b: Scheme of the normal microanatomy of the pyloric gland mucosa. Notice the relation of the marginal crypt epithelium (MCE) and subepithelial capillaries (SE). The crypt openings are not visualized at the surface. Scheme from Prof. Kenshi Yao, reference 31.
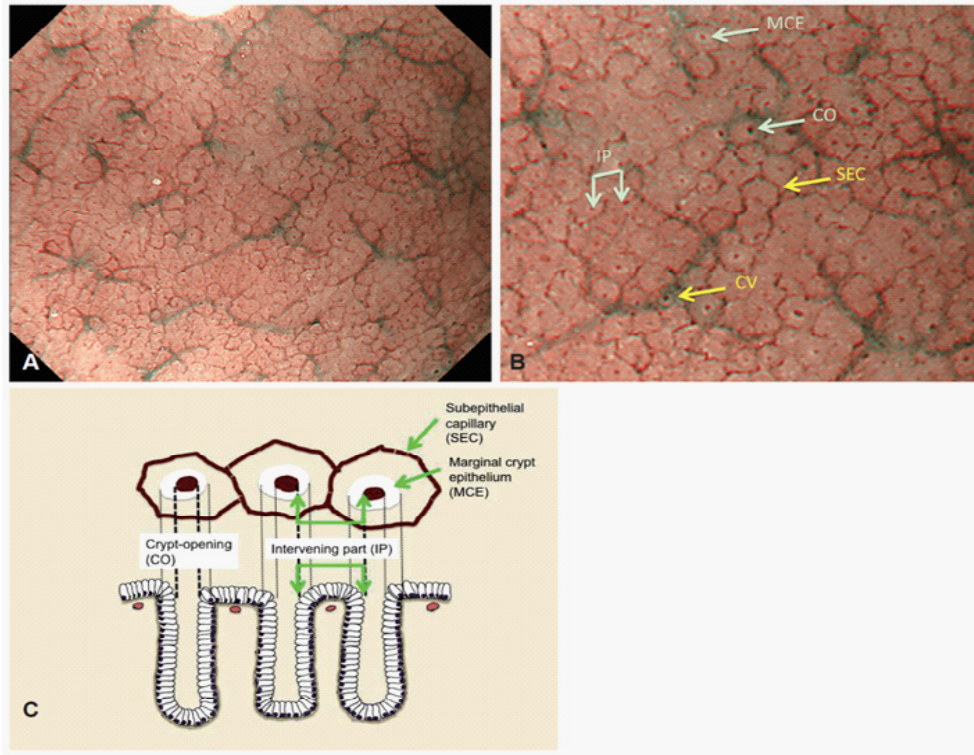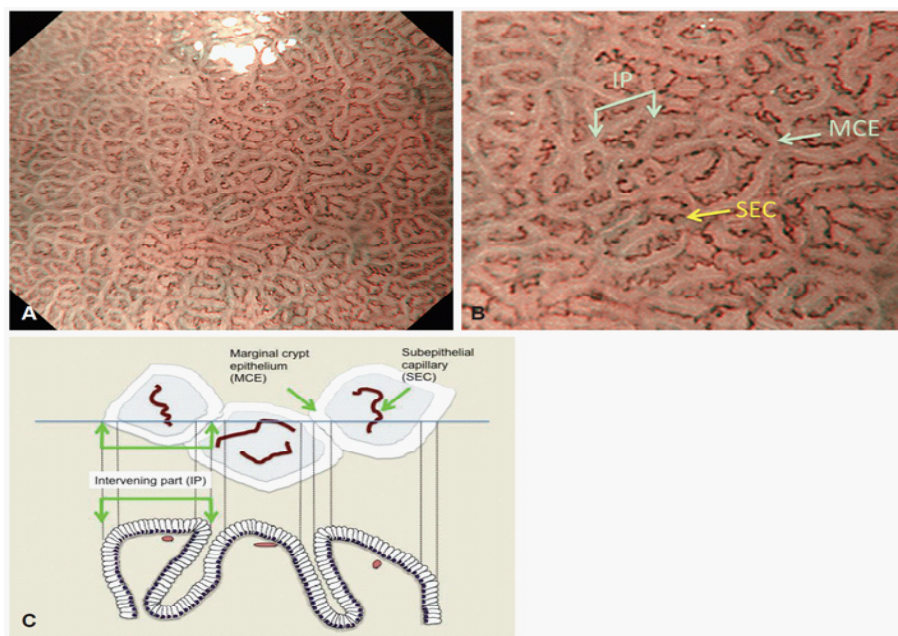
Figure 6:

A. Normal gatric fundic gland mucosa microanatomy under NBI (narrow-band imaging) magnifying observation.

B. Microvascular architecture: honeycomb-like subepithelial capillary network (SECN) and collecting venules (CV). Microsurface structure: oval crypt opening (CO) in dark brown and white circular marginal crypt epithelium (MCE). The area between crypt and crypt is called the intervening part (IP).

C. Scheme of the correlation between visualized endoscopic mucosa microanatomy and histological findings.

Reproduced from Prof. Kenshi Yao, reference 25.

Figure 7:

A. Normal gastric pyloric gland mucosa microanatomy under NBI (narrow-band imaging) magnifiing observation.

B. Microvascular architecture: coil-shaped subepithelial capillary (SEC). The collecting venules are difficult to discern because they are located in the deeper part of the lamina propria mucosae.

Microsurface structure: regular polygonal or curved marginal crypt epithelium (MCE). Crypt opening is not visualized. The intervening part (IP) is surrounded by the MCE.

C. Scheme of the correlation between visualized endoscopic mucosa microanatomy and histological findings.

Reproduced from Prof. Kenshi Yao, reference 25.
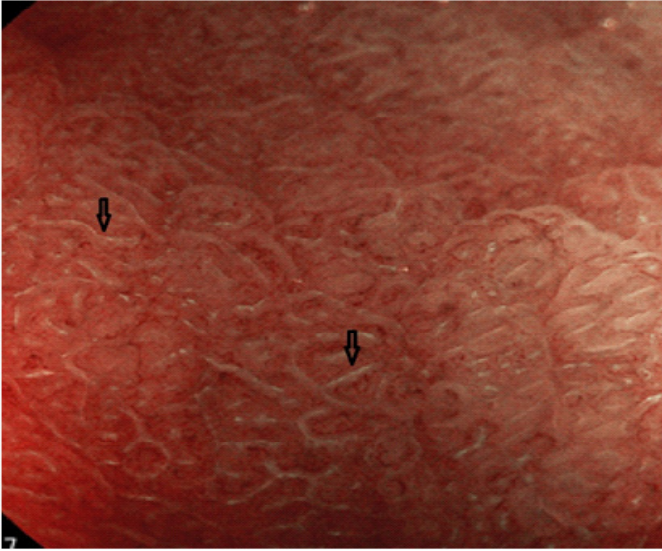
Figure 8a: Light blue Crest (LBC) sign. Numeorus fine bluish (light cyan) lines are seen in the antrum, as for example, those signalized by arrows. This phenomenon (reflection of the blue light) is characteristic of intestinal metaplasia in the stomach, but is also present in the normal mucosa of the small bowel, as seen in duodenum or ileum. Picture from Dr. Uchima, Teknon Medical Center.
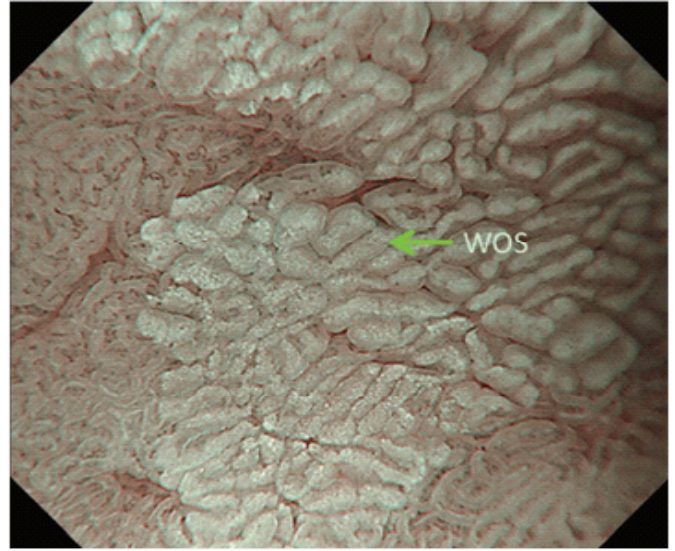

Figure 8b: White Opaque Substance (WOS). NBI (narrow-band imaging, Olympus) magnifying observation of the gastric mucosa showing an white opaque coloration (arrow) due to light strong scattering and reflection, it is produced by accumulation of lipid droplets within the surface epithelium in the stomach. Picture from Prof. Kenshi Yao, reference 23.
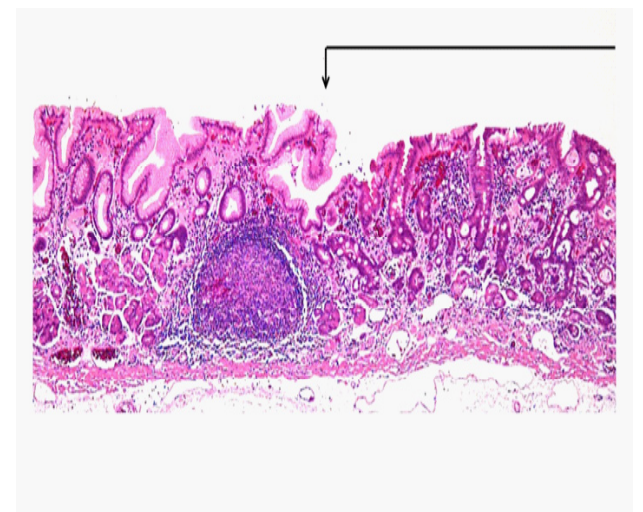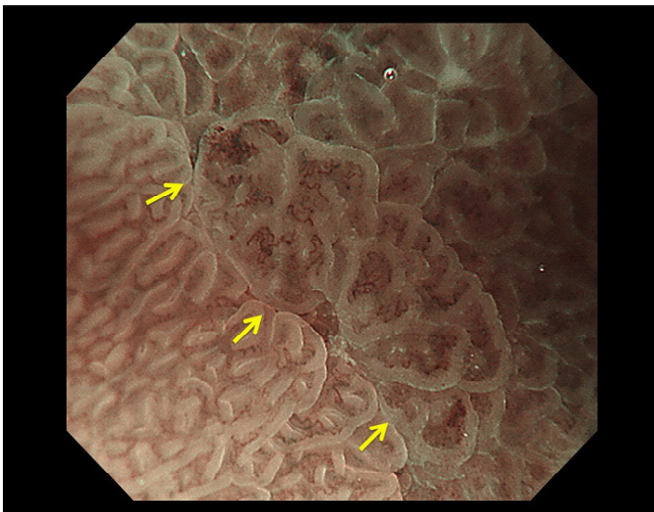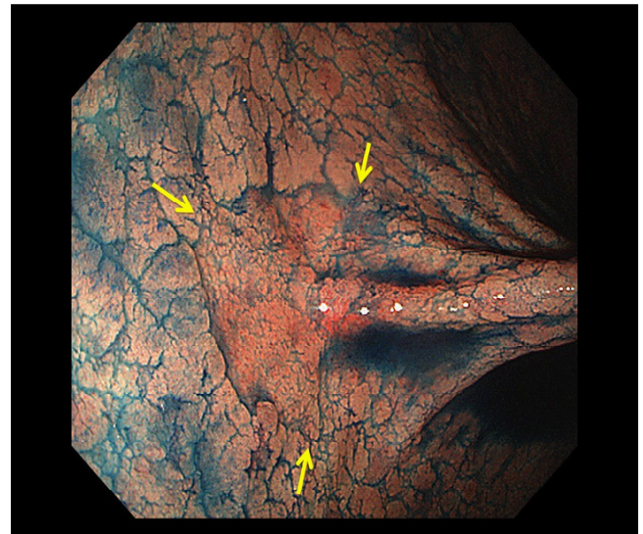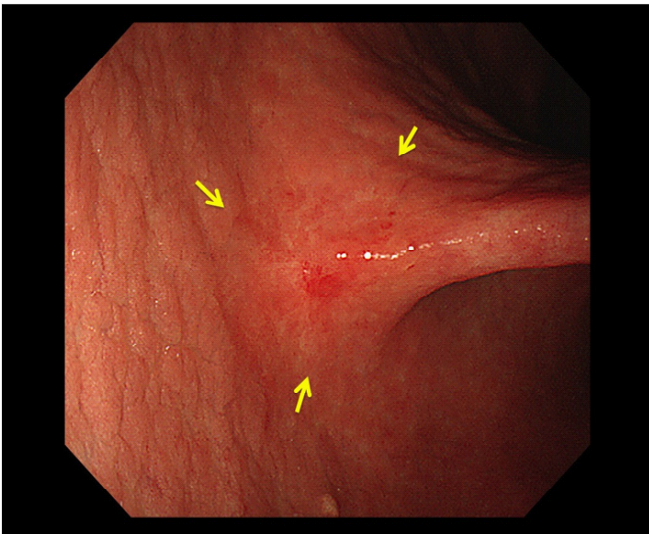
Figure 9: Demonstrable case of cancerous lesion. (a) Conventional endoscopic findings with white-light imaging. A slightly depressed lesion with discoloration (arrows) is noted at the anterior wall of the gastric angle. (b) Conventional white-light endoscopic findings with the dye (indigocarmine)- spraying method. After the dye is sprayed, the subtle lesion can be clearly visualized. As the margin of the lesion (arrows) shows irregularity, this lesion can be diagnosed as cancer. (c) Magnifying endoscopic findings with narrow-band imaging. A clear demarcation line (arrows) is noted at the margin of the lesion. Because both irregular microvascular and irregular microsurface patterns are present within the demarcation line, this lesion can be diagnosed as cancer. (d) Histological findings of endoscopically resected specimen shows well- to poorly differentiated adenocarcinoma limited to themucosa. Arrow shows the horizontal extent of the cancerous tissue. From reference 31.
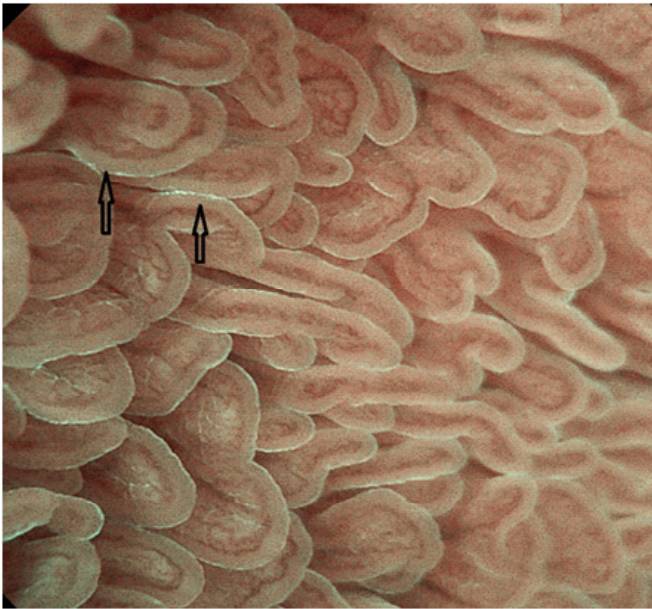

Figure 9a. Normal duodenal mucosa under BLI (Blue light imaging) magnifying observation. The blue light crest (LBC) is present (arrows). Picture Dr. Uchima, Teknon Medical Center.
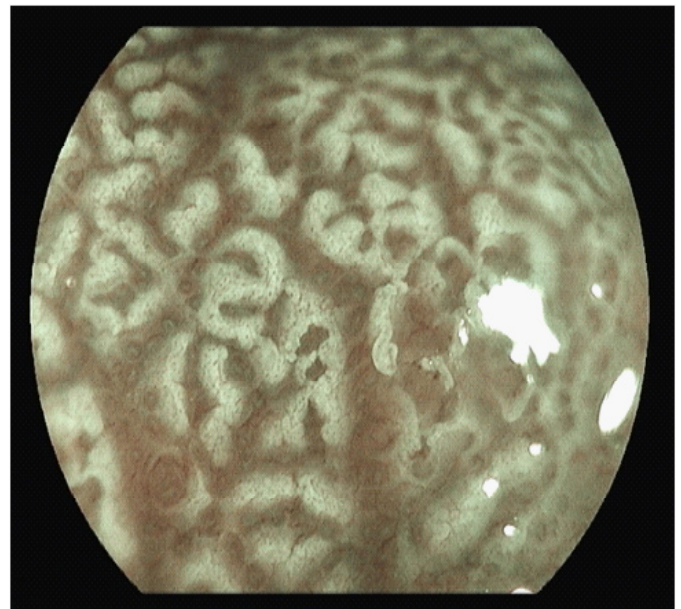

Figure 9b. Atrophy of duodenal villi under BLI (Blue light imaging) magnifying observation. Loss of microsurface structure (absence of villi). Picture Dr. Uchima, Teknon Medical Center.
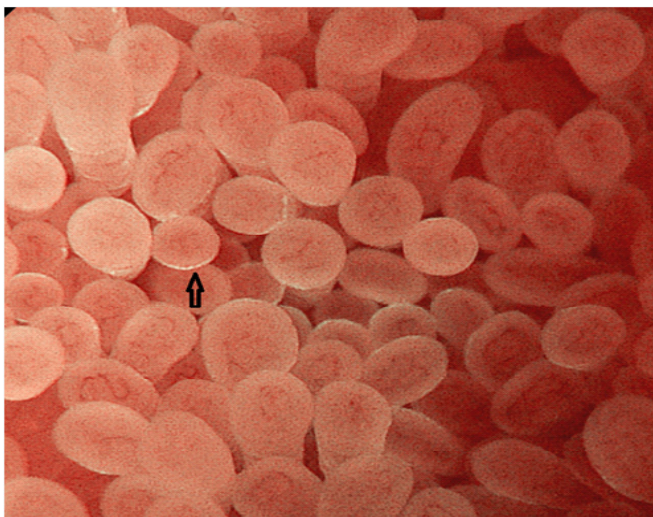

Figure 10: Normal mucosa of ileum, under BLI (Blue light imaging) magnifying observation. The blue light crest (LBC) is present (arrow). Picture Dr. Uchima, Teknon Medical Center.
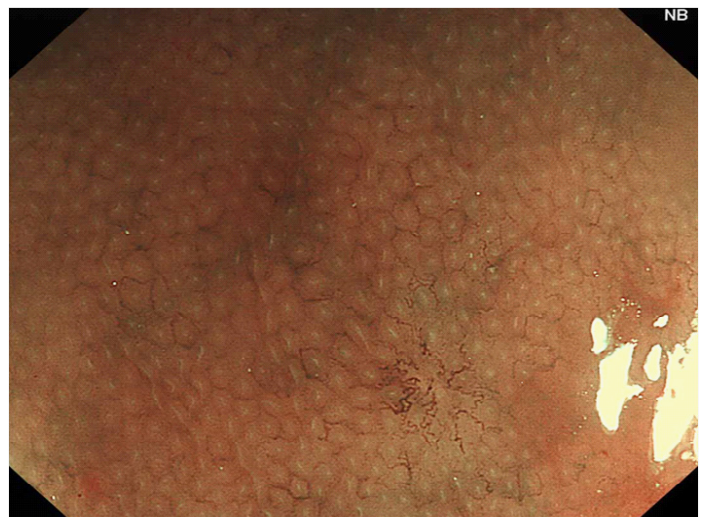

Figure 11: Honeycomb-like appearance of the subepithelial capillary network in colon, under M-DWI. Picture from Prof. Kenshi Yao, Fukuoka University Chikushi Hospital.

Figure 12: Tubular adenoma (polyp) of the colon under BLI (Blue light imaging) low magnifying observation. Regular tubular structure.

9. References

1. Peery A, Crockett S, Barritt A, Dellon E, Eluri S, Gangarosa L, et al. Burden of Gastrointestinal, Liver, and Pancreatic Diseases in the United States. Gastroenterology. 2015; 149(7): 1731–41.e3.

2. Sepanlou SG, Malekzadeh F, Delavari F, Naghavi M, Forouzanfar MH, Moradi-Lakeh M, et al. Burden of Gastrointestinal and Liver Diseases in Middle East and North Africa: Results of Global Burden of Diseases Study from 1990 to 2010A. Middle East J Dig Dis. 2015; 7(4): 201–215.

3. World Health Organization . Global health estimates 2015 summary tables:global deaths by cause, age and sex, 2000-2015.

4. OMS (IARC). Available from: http://globocan.iarc.fr/Default.aspx [Accessed 11th March 2017]

5. Lee EY, Bourke MJ. EMR should be the first-line treatment for large laterally spreading colorectal lesions. Gastrointest Endosc. 2016; 84(2): 326–328.

6. Saito Y, Sakamoto T, Nakajima, T, MatsudaT.Colorectal ESD: current indications and latest technical advances.Gastrointest Endosc Clin N Am. 2014; 24(2): 245-255.

7. Rizvi QU, Balachandran A, Koay D, Sharma P, Singh R. Endoscopic Management of Early Esophagogastric Cancer. Surg Oncol Clin N Am. 2017; 26(2): 179-191.

8. Hall J. The Eye: II. Receptor and Neural Function of the Retina. In:Hall J (ed). Guyton and Hall Textbook of Medical Physiology.Thirteenth Edition. United States of America: Elsevier; 2016.p. 647-660

9. Connors BW. Sensory Transduction. In: Boron W (ed). Medical Physiology.Third Edition.UK: Elsevier Inc.; 2017.p. 353-389.

10. Orchard GE. Pigments and minerals. In: Suvarna K, Layton C, Bancroft J (eds). Bancroft's Theory and Practice of Histological Techniques.Seventh Edition.UK: Elsevier Ltd; 2017.p. 239-270.

11. Yao K, Takaki Y, Matsui T, Iwashita A, Anagnostopoulos GK, Kaye P, et al. Clinical Application of Magnification Endoscopy and Narrow-Band Imaging in the Upper Gastrointestinal Tract: New Imaging Techniques for Detecting and Characterizing Gastrointestinal Neoplasia. Gastrointest Endosc Clin N Am. 2008;18(3): 415–433.

12. Gono K. Narrow band imaging: Technology basis and research and development history. Clin Endosc. 2015; 48(6): 476–480.

13. Du Le V, Wang Q, Gould T, Ramella-Roman J, Pfefer J. Vascular contrast in narrow-band and white light imaging. Appl Opt. 2014; 20; 53(18): 4061-4071

14. Kaneko K, Oono Y, Yano T, Ikematsu H, Odagaki T, Yoda Y,et al. Effect of novel bright image enhanced endoscopy using blue laser imaging (BLI) . Endosc Int Open. 2014; 2(4): E212-E219

15. Neumann H, Fujishiro M, Wilcox M, Mönkemüller K. Present and future perspectives of virtualchromoendoscopy with i-scan and optical enhancementtechnology. Dig Endosc. 2014; 26(Suppl. 1): 43–51

16. Tajiri H, Kato M, Tanaka S, Saito Y, Muto M. NBI/BLI Atlas. Tokyo: Nihon Medical Center; 2014.

17. Nagao M, Nishikawa J, Ogawa R, Sasaki S, Nakamura M, Nishimura J, et al. Evaluation of the Diagnostic Ability of Optical Enhancement System in Early Gastric Cancer Demarcation. Gastroenterol Res Pract. 2016; 2016: 2439621.

18. Yabe H. Magnifying ratio and resolution of electronic endoscopes.Dig Endosc. 2002; 14 Suppl 1: S88–90.

19. Yao K. Zoom Gastroscopy. Tokyo: Springer; 2014.

20. Kumagai Y, Toi M, Inoue H. Dynamism of tumour vasculature in the early phase of cancer progression: outcomes from oesophageal cancer research. Lancet Oncol. 2002; 3(10): 604-610

21. Shepherd N, Warren B, Williams G, Greenson J, Lauwers G, Novelli M. Morson and Dawson's gastrointestinal pathology. 5th ed. London: Blackwell Publishing; 2013.

22. Inoue H, Kaga M, Ikeda H, Sato C, Sato H, Minami H, et al. Magnification endoscopy in esophageal squamous cell carcinoma : a review of the intrapapillary capillary loop classification. Ann Gastroenterol. 2015; 28(1): 41–48.

23. Inoue H, Honda T, Yoshida T, Nishikage T, Nagahama T, Yano K et al. Ultra-high Magnification Endoscopy of the Normal Esophageal Mucosa. Dig Endosc.1996; 8: 134–138.

24. Sharma P, Bergman JJGHM, Goda K, Kato M, Messmann H, Alsop BR, et al. Development and Validation of a Classification System to Identify High-Grade Dysplasia and Esophageal Adenocarcinoma in Barrett's Esophagus Using Narrow-Band Imaging. Gastroenterology. 2016; 150(3): 591–598.

25. Yao K. Clinical application of magnifying endoscopy with narrow-band imaging in the stomach. Clin Endosc. 2015; 48(6): 481–490.

26. Uedo N, Ishihara R, Iishi H, Yamamoto S, Yamada T, Imanaka K, et al. A new method of diagnosing gastric intestinal metaplasia: narrow-band imaging with magnifying endoscopy. Endoscopy. 2006; 38(8): 819–824

27. Yao K, Iwashita A, Tanabe H, Nishimata N, Nagahama T, Maki S et al. White opaque substance within superficial elevated gastric neoplasia as visualized by magnificationendoscopy with narrow-band imaging: a new optical sign for-differentiating between adenoma and carcinoma. GastrointestEndosc. 2008; 68(3): 574–580.

28. Yao K, Iwashita A, Nambu M, Tanabe H, Nagahama T, Maki S, et al. Nature of white opaque substance in gas-tric epithelial neoplasia as visualized by magnifying endoscopy with narrow-band imaging. Dig Endosc.2012; 24(6): 419–425.

29. Enjoji M, Kohjima M, Ohtsu K, Matsunaga K, Murata Y, Nakamuta M, et al. Intracellular mechanisms underlying lipid accumulation (white opaque substance) in gastric epithelial neoplasms : A pilot study of expression pro fi les of lipid-metabolism-associated genes. J Gastroenterol Hepatol. 2016; 31(4): 776–781.

30. Kanemitsu T, Yao K, Nagahama T, Imamura K, Fujiwara S, Ueki T, et al. Extending magnifying NBI diagnosis of intestinal metaplasia in the stomach: the white opaque substance marker. Endoscopy. 2017; 49(6): 529-535

31. Muto M, Yao K, Kaise M, Kato M, Uedo N, Yagi K, et al. Magnifying endoscopy simple diagnostic algorithm for early gastric cancer (MESDA-G). Dig Endosc. 2016; 28(4): 379–393.

32. Yao K. Normal duodenal mucosa. In: Muto M, Yao K, Sano Y ed. Atlas of endoscopy with narrow band imaging. Tokyo, Japan: Springer. 2015 p.147.

33. De Luca L, Ricciardiello L, Rocchi MB, Fabi MT, Bianchi ML, de Leone A, et al. Narrow band imaging with magnification endoscopy for celiac disease: results from a prospective, single-center study. Diagn Ther Endosc. 2013; 2013: 580526.

34. Dutta AK, Sajith KG, Shah G, Pulimood AB, Simon EG, Joseph AJ, et al. Duodenal villous morphology assessed using magnification narrow band imaging correlates well with histology in patients with suspected malabsorption syndrome. Dig Endosc. 2014; 26(6): 720–725.

35. Singh R, Nind G, Tucker G, Nguyen N, Holloway R, Bate J, et al. Narrow-band imaging in the evaluation of villous morphology: A feasibility study assessing a simplified classification and observer agreement. Endoscopy. 2010; 42(11): 889–894.

36. Yao K, Anagnostopoulos GK, Jawhari AU, Kaye P V, Hawkey CJ, Ragunath K. Optical Microangiography : High-Definition Magnification Colonoscopy with Narrow Band Imaging (NBI) for Visualizing Mucosal Capillaries and Red Blood Cells in the Large Intestine. Gut and Liver. 2008; 2(1): 14–18.

37. Sano Y, Tanaka S, Kudo SE, Saito S, Matsuda T, Wada Y, et al. Narrow-band imaging (NBI) magnifying endoscopic classification of colorectal tumors proposed by the Japan NBI expert team. Dig Endosc. 2016; 28(5): 526–533.

38. Uraoka T, Saito Y, Ikematsu H, Yamamoto K, Sano Y. Sano's capillary pattern classification for narrow-band imaging of early colorectal lesions. Dig Endosc. 2011; 23(SUPPL 1): 112–115.

39. Ikematsu H, Matsuda T, Emura F, Saito Y, Uraoka T, Fu K-I, et al. Efficacy of capillary pattern type IIIA/IIIB by magnifying narrow band imaging for estimating depth of invasion of early colorectal neoplasms. BMC Gastroenterol. 2010; 10: 33.